inter.noise
21-24 AUGUST
SCOTTISH EVENT CAMPUS
GLASGOW 2022

The effect of the vibrissa shaped cylinder on the aeolian tone mitigation

Guanjiang Chen [1], Xiao Liu [2], Bin Zang[3], Mahdi Azarpeyvand[4]

Faculty of Engineering, University of Bristol, United Kingdom, BS8 1TR

ABSTRACT

This paper studies vibrissa shaped cylinder as a passive control method for reducing the aerodynamic noise of the flow past a cylinder. One elliptical cylinder and a circular cylinder are also investigated for comparison. The far-field noise results show that compared with the circular cylinder case, the tonal peak almost disappears in the vibrissa shaped cylinder case and the sound pressure level (SPL) could be reduced by about 20dB at Re≈36,000. The elliptical cylinder only shows a slight SPL reduction by about 4 dB with a shift in the tonal peak frequency from St=0.2 to St=0.36. Furthermore, some noticeable variations occur in the noise directivity pattern for the vibrissa shaped cylinder case. The shift in the tonal peak frequency, the reduction in noise and modifications in the noise directivity are related to the changing and breakdown of the vortex shedding caused by the interference with the elliptical and vibrissa shaped cylinder surfaces. The PIV experiments are conducted to the three cases for the flow field information to further understand the mechanism of the noise reduction caused by the vibrissa shaped cylinder and the elliptical cylinder.

1. INTRODUCTION

Flow past a bluff body is a frequently encountered topic in aerodynamic and aeroacoustic research due to its extensive engineering application. Circular cylinder is the basic model for the bluff body, which has been studied in many previous works. Revell, et al. [1] built the relationship between sound pressure level (SPL) and drag coefficient (C_d) experimentally for the Reynolds number range from 45,000 to 450,000. Alemaroglu, et al. [2] used acoustic pressure measurements and hot wire velocity measurements to study the relationship between the far field acoustic pressure and the surface boundary layer condition. The coherence at the fundamental vortex shedding frequency was intense in the subcritical and the supercritical regimes, while the value became low in the transcritical regime. Through cross-correlation analysis, Oguma, et al. [3] experimentally evaluated that the sound sources were near both separation points of two sides of the cylinder and in the near wake. The simulation work of Orselli, et al. [4] used the CFD/acoustic analogy method to get the near field and far field pressure results. With the correction method of Kato, et al.[5], the SPL calculated from the 3-D LES matched well with the experiment of Ref. [1]. Lysenko, et al. [6] simulated the flow past a cylinder using LES and concluded that the sound source had a dipole nature. More studies could be found in reviews of Blevins [7] and Porteous, et al. [8] .

For the sake of environment protection, studies about the noise mitigation are of great concern. [9, 10]. Two classes of methods are usually adapted to reduce the noise: the active flow control, which

[1] PhD Student, Department of Aerospace Engineering, guanjiang.chen@bristol.ac.uk

[2] Technical Specialist, Wind Tunnel Laboratory, xiao.liu@bristol.ac.uk

[3] Lecturer in Aeroacoustics, Department of Aerospace Engineering, nick.zang@bristol.ac.uk

[4] Professor of Aerodynamics and Aeroacoustics, Department of Aerospace Engineering, m.azarpeyvand@bristol.ac.uk

changes the flow structure using energy inputs; the passive flow control, which modifies the geometry. Compared with the active flow control methods which usually introduce extra flow [11, 12], the passive flow control methods such as using the porous medium and the geometry modification are more robust. The porous medium could mitigate the interaction between the fluid and solid surface. [10, 13-15]. The geometry modification introduces various disturbances [9] or changes the surface shape to alter the near wall flow structures and will reduce the flow-induced noise [16], which is easy to be implemented. This paper focused on a bio-inspired shape based on Harbour Seals' vibrissa, which is reported to change the vortex shedding process and reduce the vibration [17].

There has been some research about the flow past a vibrissa shaped cylinder. Wang and Liu[18] experimentally studied the wake behind a vibrissa shaped cylinder through time-resolved particle image velocity. The vortex shedding process of the vibrissa cylinder was disrupted by the irregular surface, which suppressed the vortex-induced vibration. Kim and Yoon [19] conducted LES for the flow past an elliptical cylinder and the flow past a vibrissa cylinder. The shear layer of the vibrissa case was much longer than that of the elliptical case. When the angle of the attack increased, two flow structures between the vibrissa case and the elliptical case became similar because the bluff body flow overcame the flow induced by the vibrissa cylinder. Jie and Liu [20] simulated the flow past a vibrissa cylinder using LES. The results showed the fluctuation of lift force is reduced by approximately 79.2% for the vibrissa case compared with the circular cylinder case. The POD analysis revealed the wake shedding processes on the nodal and saddle planes are not synchronous. The flow structure near the vibrissa cylinder results in smaller velocity and pressure fluctuations. The LES research of Chu, et al.[21] also showed the flow past a vibrissa cylinder presented the three-dimensional separation, and the out-phase vortex shedding on the nodal and saddle planes made a significantly influenced the lift fluctuation.

In summary, most research on the flow past a vibrissa cylinder focus on the aerodynamic characteristics, and it is worthwhile to study the noise reduction effects of the vibrissa cylinder. Detailed aerodynamic characteristics and noise performances of a circular cylinder, an elliptical cylinder and a vibrissa cylinder are presented in this paper. Furthermore, the PIV measurements are conducted for the near flow field results, which contributes to a better understanding of noise reduction mechanism of the vibrissa cylinder.

2. EXPERIMENTAL SETUP

The far-field noise measurement and the near-field PIV measurement are conducted on the flow past different cylinders with the freestream velocity at 25m/s with the Reynolds number $Re \approx 36{,}000$ based on the cylinder diameter D. The detail configurations of cylinder models are shown in Table 1 and Fig. 1. The circular cylinder with diameter D=22mm is used as the baseline case. The elliptical cylinder and the vibrissa cylinder are designed to make sure they have similar volumes with the circular cylinder, and their ratios between major and minor axes are close.

Table 1: Geometrical parameters of the cylinders.

	D	λ	a_e	b_e	α	β	A_v	B_v	a_v	b_v
Circular	22									
Elliptical			7.7	15.7						
Vibrissa		27.5			15.27	17.6	7.26	17.82	8.58	14.3

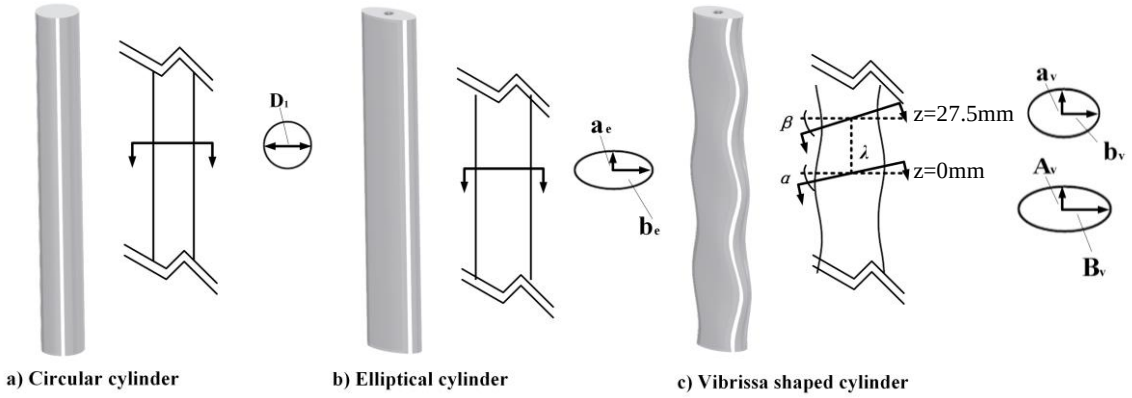

Figure 1 : Cylinder geometries in this study

2.1. Far-field noise measurement

The experiments are performed in the aeroacoustic wind tunnel facility at University of Bristol [22]. Figure 2(a) shows the images of the wind tunnel with the cylinder test set-up. The test section is connected with a nozzle of 500 mm width and 775 mm height. Far-field noise measurements are conducted using an array of microphones mounted on an arc, positioned 1.75m far away from the experimental model. The origin is set at the center of the mid-span cross-section of the cylinder, and the X direction is the streamwise direction.

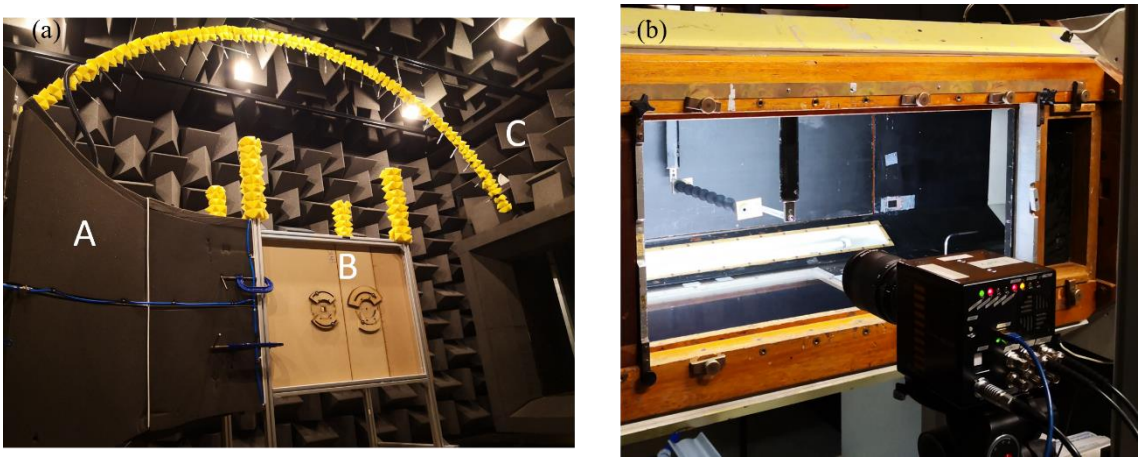

Figure 2 : (a) Photograph of the anechoic chamber including A. Nozzle, B. Test section, C. far-field microphone; (b) photograph of the low turbulence wind tunnel and the PIV measurement setup

2.2. PIV measurement

The flow field around cylinder are studied using two-dimensional two-component Particle Image Velocimetry (PIV) in the low turbulence closed circuit wind tunnel, as shown in Fig.2(b). A total of 2000 images for each measurement are captured at a frequency of 840Hz, using a Photron FASTCAM Mini WX 100 camera with a resolution of 2048 × 2048 pixels^2 and 14 bit image depth. The images were analyzed using multi-pass cross-correlation algorithm with a final window of 32 × 32 pixels^2 and 50% overlap in LaVision DaVis software, which corresponds to a resolution of 132mm × 106mm in the vector field.

3. RESULTS AND DISCUSSION

3.1. Sound Pressure Level

Figure 3(a) shows the far-field SPL at θ=90º with freestream velocity U_∞=25m/s. Note that θ=0º points to the upstream, while θ=180º points to the downstream. Overall, the SPL value decreases with the Strouhal number St (St=fD/U_∞, where f is frequency), and the SPL values of three cases are close when St is higher than 0.3. For the circular cylinder case, the tonal peak with a protrusion of 20dB from the broadband component is well captured at St=0.19, which is close to the theoretical fundamental vortex shedding frequency. A peak at the second harmonic occurs in the circular cylinder case at St=0.58 with much smaller protrusion compared with the major peak at St=0.19. The elliptical cylinder case shows a tonal peak at St=0.36, which means the fundamental vortex shedding frequency of the elliptical cylinder case experiences a shift from the value of the circular cylinder case. Furthermore, there is no peak at the first and second harmonics of the elliptical cylinder case. A noise reduction of 4dB could been seen for the for the tonal component of the elliptical cylinder case compared with the circular cylinder case. A more obvious reduction of tonal peak value appears in the vibrissa cylinder case, which just shows a small bump at around St=0.25, and there is no peak at harmonics. As a results, the vibrissa cylinder mitigates the noise significantly, though its SPL value is a little higher than the other two cases when St smaller than 0.12.

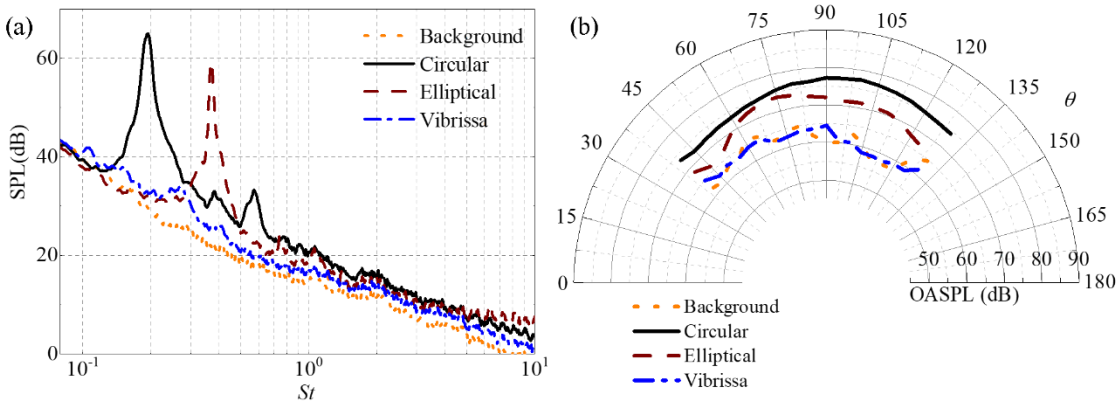

Figure 3 : (a) Far-field SPL at θ=90º; (b) OASPL for all cases with U_∞=25m/s

3.2. Overall sound pressure level

Figure 3(b) shows the overall sound pressure level (OASPL) and the directivity pattern for the circular cylinder, elliptical cylinder, and vibrissa cylinder cases. Only the OASPL from θ=40º to θ=130º is presented due to the space limitation. The OASPL value of the elliptical cylinder case is smaller than that of the circular cylinder case, which is consistent with the SPL value reduction in Fig.3(a). Near θ=75º, the OASPL value of the elliptical cylinder case exhibits an increased noise level. The reason of which may be the wind tunnel inlet effect or the changes to the directivity pattern, which need further investigations in the future. The changes of the OASPL value with angles are also obvious for the vibrissa cylinder case, which is strongly influenced by the background noise. Nevertheless, the vibrissa cylinder case shows significant smaller OASPL values at all angles than the other two case because of the mitigation of its tonal components.

3.3. Flow field

Figure 4 shows the instantaneous streamwise velocity contours in the x-y plane. For the circular cylinder case and the elliptical cylinder case, the mid plane in the spanwise direction is chosen, while for the vibrissa cylidner case, the saddle plane at z=0mm and the nodal plane at z=27.5mm are presented, as shown in Fig.1. Note that in this section Y/D=0 is the centerline of cylinder and X/D=0 is the line just behind the cylinder. For the circular cylinder case, the vortex shedding is captured, and the wake expands along the flow direction. The wake expansion of the elliptical cylinder case is not as obvious as the cylinder case, and the vortex shedding is more frequent for the elliptical cylinder case, which is related to higher fundamental vortex shedding frequency as shown in Fig.3(a). For the vibrissa cylinder case, the vortex shedding is not obvious. The wake size in the saddle plane (z=0mm) is smaller than that in the nodal plane(z=27.5mm), and the wake expansions of the vibrissa case are weaker than that of the cylinder case, causing less disturbances in the far-field.

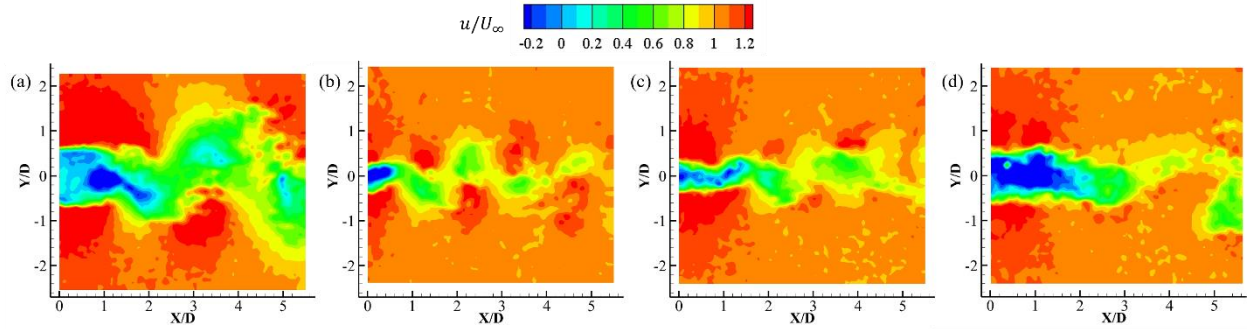

Figure 4 : Instantaneous streamwise velocity field in the x-y plane of (a) the circular cylinder, (b) the elliptical cylinder, the vibrissa cylinder (c) at the z=0mm, and (d) at the z=27.5mm.

Figure 5 and 6 show time-averaged streamwise velocity contours on the x-y plane and the time-averaged streamwise velocity along the center line (Y/D=0). The mid planes of the circular cylinder case and the elliptical cylinder case are presented, while four planes from z=0mm to z=41.25mm are exhibited for the vibrissa cylinder case. For the circular cylinder case, a big recirculation region occurs just behind the cylinder, and the recirculation bubble length is about 1.5D as shown in Fig.6 which is consistent with the literature data in Ref. [23]. The elliptical cylinder case shows much smaller recirculation region and wake size than the circular cylinder case, contributing to less disturbances in the far-field. The velocity distributions changes along the spanwise direction for the vibrissa cylinder case. The recirculation region is very small in the saddle plane at z=0mm, and it is obvious in the nodal plane at z=27.5mm. It can be seen from figure 6 that the mean streamwise velocity distributions of the center line exhibit great differences in the spanwise direction of the vibrissa cylinder case. The velocity value is relatively high in the saddle plane and low in the nodal plane when X/D is smaller than 5.5. The velocity value at other planes, i.e. z=13.75mm and z=41.25mm, are within the range between the saddle plane value and the nodal plane value, while the size of recirculation region and wake shows similar phenomenon as shown in Fig.5. These differences along the spanwise direction indicate that the coherence of the flow structure for the vibrissa cylinder case is low, and its vortex shedding process is more three-dimensional, causing weaker far-field acoustic pressure fluctuation and lower noise level than the other two cases.

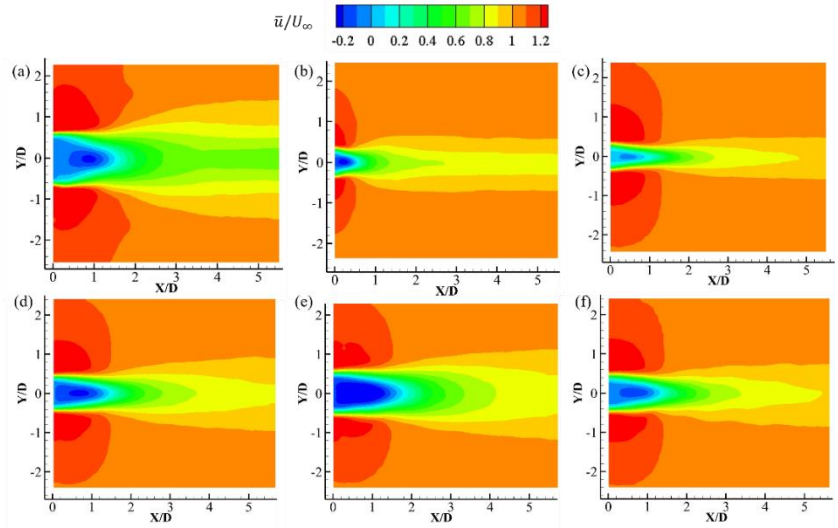

Figure 5 : Time-averaged streamwise velocity field in the x-y plane of (a) the circular cylinder, (b) the elliptical cylinder, the vibrissa cylinder (c) at the z=0mm plane, (d) at the z=13.75mm plane, (e) at the z=27.5mm plane, and (f) at the z=41.25mm plane.

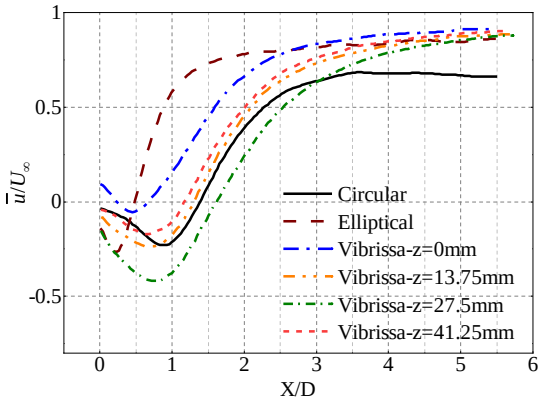

Figure 6 : Time-averaged streamwise velocity in the center line (Y/D=0)

3.4. Velocity power spectral density

The power spectral density (PSD) of streamwise velocity from the PIV results is presented in Fig.7. The studied probes are in the mid plane of the circular cylinder case and the elliptical cylinder case, while for the vibrissa cylinder case, the probes are in the saddle plane at z=0mm and the nodal plane at z=27.5mm. The position of shear layer line is different according to the cylinder, which is Y/D=0.5 for the circular cylinder, Y/D=0.35 for the elliptical cylinder, and Y/D=0.39 for the vibrissa cylinder respectively. The PSD calculation is conducted by the '*Pwelch*' function in Matlab. The velocity PSD data are referenced to 25m/s. Overall, the PSD value in the shear layer line is higher than that in the line of Y/D=1, indicating stronger velocity fluctuation. The broadband components of the elliptical cylinder case and vibrissa cylinder case are smaller than that of the circular cylinder case, except for the probe in the shear layer of the nodal plane of the vibrissa case. The reason of which is that the elliptical cylinder and the vibrissa cylinder cases cause smaller vortices and weaker velocity fluctuations than the circular cylinder case. An obvious tonal peak appears in the circular cylinder case at the fundamental vortex shedding frequency at St=0.19, which is consistent with the SPL results in

section 3.1. The elliptical cylinder case also shows a tonal peak at St=0.35, at almost the same frequency with its major SPL peak. It can be concluded that the frequency of the major SPL peak is the same with the near-field vortex shedding frequency. For the vibrissa cylinder case, a tonal peak with relatively small protrusion occurs at St=0.25 in the nodal plane, and there is no tonal peak in the saddle plane. As a result, the SPL of the vibrissa cylinder case just shows a small bump near St=0.25. The low-correlated vortex shedding and the small tonal peak value induce much less noise level for the vibrissa cylinder case than its counterparts.

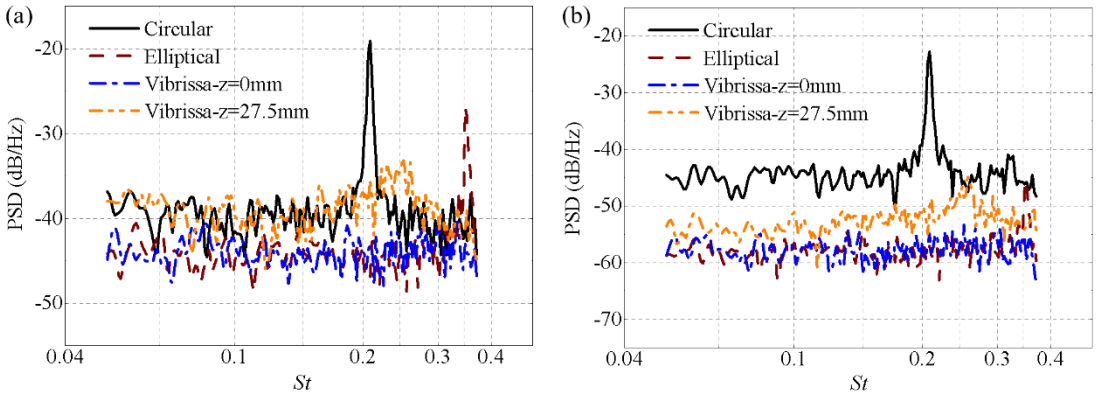

Figure 7 : Velocity power spectral density for all cases at X/D =2 in (a) the shear layer line and (b) the line of Y/D=1.

4. CONCLUSIONS

The far-field noise measurement and the near-field PIV measurement are conducted to study the aeroacoustic performance of the flow past a vibrissa cylinder. A circular cylinder case and an elliptical cylinder case are also investigated for comparison. Compared with the circular cylinder case, the elliptical cylinder case shows a shift in the tonal peak frequency from St=0.2 to St=0.36 as well as a 4dB reduction for the SPL tonal peak value, resulting in a smaller overall sound pressure level (OASPL). The SPL tonal peak almost disappears in the vibrissa case with just a small bump around St=0.25, and the OASPL value of the vibrissa cylinder case is significantly smaller than the other two cases. The sizes of vortices and the wake regions in the vibrissa cylinder and elliptical cylinder cases are smaller than that of the circular cylinder case, causing the weaker far-field acoustic pressure fluctuation and lower noise level. The frequency of the major SPL peak is the same with the vortex shedding frequency of the cylinder. The vortex shedding process of the flow past a vibrissa cylinder is less correlated along the spanwise direction. The low-correlated vortex shedding and the small tonal peak value contribute to the noise mitigation effect of the vibrissa cylinder.

5. ACKNOWLEDGEMENTS

The authors acknowledge the Fluid and Aerodynamics Research Group of University of Bristol. The first author's PhD grant is funded by the China Scholarship Council (CSC)-University of Bristol (UoB) PhD Scholarship.

6. REFERENCES

1. Revell, J.D., R.A. Prydz and A.P. Hays, Experimental study of aerodynamic noise vs drag relationships for circular cylinders. *AIAA Journal*, **16(9)**, 889-897 (1978).

2. Alemdaroğlu, N., Rebillat, J.C., Goethals, R., An aeroacoustic coherence function method applied to circular cylinder flows. *Journal of Sound and Vibration*, **69(3)**, 427-439 (1980).
3. Oguma, Y., Yamagata, T., Fujisawa, N., Measurement of sound source distribution around a circular cylinder in a uniform flow by combined particle image velocimetry and microphone technique. *Journal of Wind Engineering and Industrial Aerodynamics*, **118**, 1-11(2013).
4. Orselli, R., Meneghini, J., Saltara, F., Two and three-dimensional simulation of sound generated by flow around a circular cylinder. AIAA 2009-3270 (2009).
5. Kato, C., Ilda, A., Takano, Y., Fujita, H., Ikagawa, M., Numerical prediction of aerodynamic noise radiated from low Mach number turbulent wake. AlAA 93-0145 (1993).
6. Lysenko, D.A., Ertesvåg, I.S., Rian K.E., Towards Simulation of Far-Field Aerodynamic Sound from a Circular Cylinder Using OpenFoam. *International journal of aeroacoustics*, **13(1-2)**, 141-168 (2014).
7. Blevins, R.D., Review of sound induced by vortex shedding from cylinders. *Journal of Sound and Vibration*, **92(4)**, 455-470 (1984).
8. Porteous, R., Moreau, D.J., Doolan, C.J., A review of flow-induced noise from finite wall-mounted cylinders. *Journal of Fluids and Structures*, **51**, 240-254, (2014).
9. Li, L., Liu, P., Xing, Y., Guo, H., Experimental investigation on the noise reduction method of helical cables for a circular cylinder and tandem cylinders. *Applied Acoustics*, **152**, 79-87 (2019).
10. Yuan, Y., Xu K. and Zhao K., Numerical analysis of transport in porous media to reduce aerodynamic noise past a circular cylinder by application of porous foam. *Journal of Thermal Analysis and Calorimetry*, **141(5)**, 1635-1646 (2020).
11. Thomas, F.O., Kozlov, A. and Corke, T.C., Plasma actuators for cylinder flow control and noise reduction. *AIAA journal*, **46(8)**, 1921-1931(2008).
12. Al-Sadawi, L.A. and T.P. Chong. Circular cylinder wake and noise control using DBD plasma actuator. AIAA 2019-2759 (2019).
13. Geyer, T.F., Vortex shedding noise from finite, wall-mounted, circular cylinders modified with porous material. *AIAA Journal*, 2020. 58(5): p. 2014-2028.
14. Arcondoulis, E.J., Liu, Y., Li, Z., Yang, Y., Wang, Y., Structured porous material design for passive flow and noise control of cylinders in uniform flow. *Materials*, **12(18)**, 2905, (2019).
15. Xu, C., Mao Y., and Hu, Z., Control of cylinder wake flow and noise through a downstream porous treatment. *Aerospace Science and Technology*, **88**, 233-243 (2019).
16. Duan, F. and Wang, J., Fluid–structure–sound interaction in noise reduction of a circular cylinder with flexible splitter plate. *Journal of Fluid Mechanics*, **920**, (2021).
17. Hanke, W., Witte, M., Miersch, L., Brede, M., Oeffner, J., Michael, M., Hanke, F., Leder, A., and Dehnhardt, G., Harbor seal vibrissa morphology suppresses vortex-induced vibrations. *Journal of Experimental Biology*, **213(15)**, 2665-2672 (2010).
18. Wang, S. and Liu, Y., Wake dynamics behind a seal-vibrissa-shaped cylinder: a comparative study by time-resolved particle velocimetry measurements. *Experiments in Fluids*, **57**, 32 (2016).
19. Kim, H. and Yoon, H.S., Effect of the orientation of the harbor seal vibrissa based biomimetic cylinder on hydrodynamic forces and vortex induced frequency. *AIP Advances*, **7(10)**, 105015 (2017).
20. Jie, H. and Liu, Y.Z., Large eddy simulation and proper orthogonality decomposition of turbulent flow around a vibrissa-shaped cylinder. *International Journal of Heat and Fluid Flow*, **67**, 261-277 (2017).
21. Chu, S.J., Xia, C., Wang, H., Fan, Y., Yang, Z., Three-dimensional spectral proper orthogonal decomposition analyses of the turbulent flow around a seal-vibrissa-shaped cylinder. Physics of Fluids, **33(2)**, 025106 (2020).
22. Mayer, Y.D., Hasan, K.J., Szoke, M., Ali, S.A.S, Azarpeyvand, M., Design and performance of an aeroacoustic wind tunnel facility at the University of Bristol. *Applied Acoustics*, **155**, 358-370 (2019).
23. Molochnikov, V., Mikheev, N.I., Mikheev, A.I., Saushin, I.I., Flow structure and turbulent kinetic energy of velocity fluctuations in a cylinder near wake at Re = 3900. *Journal of Physics: Conference Series*, **1565**, 012003 (2020).